Journal of Applied Fluid Mechanics, Vol. 10, No. 2, pp. 639-649, 2017.
Available online at www.jafmonline.net, ISSN 1735-3572, EISSN 1735-3645.
DOI: 10.18869/acadpub.jafm.73.239.26702

A New Formulation for Prediction of Permeability of Nano Porous Structures using Lattice Botzmann Method

M. Mostafavi[1] and A. H. Meghdadi Isfahani[1†]

Department of Mechanical Engineering, Najafabad branch, Islamic Azad University, Najafabad, Iran

†*Corresponding Author Email: amir_meghdadi@pmc.iaun.ac.ir*

(Received June 16, 2016; accepted November 24, 2016)

ABSTRACT

The standard lattice Boltzmann equation, LBE, is inadequate for simulating gas flows in nano scale flows with Knudsen numbers higher than 0.1. In the present study, rarefied gas flow in nano porous structures is simulated using the modified Lattice Boltzmann Method, LBM, which is able to cover wide range of flow regimes. The present study, reports the effects of the Knudsen number and porosity on the flow rate and permeability in slip and transitional flow regimes. For the first time, the Knudsen's minimum effect in micro/nano porous was observed. A new correlation between the permeability, the porosity and the Knudsen number is then proposed which is able to predict the permeability of in-line and staggered nano porous structures in slip and transitional regimes.

Keywords: Lattice Boltzmann method; Nanoscale flow; Porous media; Transitional flow regime.

NOMENCLATURE

D	hydraulic diameter
Da	Darcy number
DF	darcy-Forchheimer drag
e	microscopic velocity
f	particle distribution function
H	characteristic length
h	channel height
k	permeability
Kn	Knudsen number
L	porous media length
p	pressure
Re	Reynolds number
s	slip reflection coefficient
t	time
u	x component of the velocity
v	y component of the velocity
U	average velocity
V	volume
V_s	obstacles volume
ρ	density
τ	relaxation time
ε	porosity
μ	viscosity
$\boldsymbol{\Omega}$	collision function

1. INTRODUCTION

Fluid flow and transport processes in porous media are relevant in a wide range of fields, including hydrocarbon recovery, groundwater flow, CO2 sequestration, metal foam, fuel cell, and other engineering applications (Dullien 2005). Understanding the fluid dynamics in porous media and predicting effective transport properties (permeability, effective diffusivity, etc.) is of paramount importance for practical applications (Chen *et al.* 2005, 2014).

Recent technological developments have made it possible to design various micro/nano devices such as micro/nano channels, nozzles and pumps, where fluid flow and heat transfer are involved. The extensive engineering applications of nano-scale fluid flow through porous media have popularized the wide-ranging topics related to this subject of research. In micro/nano devices, porous media can be used for micro filtration, fractionation, catalysis and microbiology related applications (Jeong *et al.* 2006). For example, micro packed beds or sintered metal fibers can be used in micro structured reactors for catalytic reaction (Yuranov *et al.* 2005, Kiwi-Minsker *et al.* 2005) and the filter medium prepared from commercially available glass fibers of 70-

$140\ \mu m$ thickness is suitable for applications in bio filtration systems (Assis *et al.* 2003). Also charged porous media structures have been employed in micro devices to magnify the pumping (Brask *et al.* 2005, Bazant *et al.* 2004), mixing (Oddy *et al.* 2001, Biddiss *et al.* 2004) and separating (Wong *et al.* 2004) effects.

Conventional numerical methods using the Navier-Stokes equations fail to predict some aspects of micro/nano flows. Flow in micro/nano scales is divided into four flow regimes based on the Knudsen number $\mathrm{Kn} = \lambda / \mathrm{L}$, which is the ratio of molecular mean free path to characteristic length scale (Karniadakis *et al.* 2005). There are two methods for definition of L in porous media. Roy *et al.* (2003) defined the hydraulic diameter of obstacles, D, as the characteristic length scale, while Kast *et al.* defined the average void diameter, D_h, as the characteristic length L. Considering the fact that the fluid flows between the obstacles, it is better to define $\mathrm{Kn} = \lambda / \mathrm{D_h}$. For $\mathrm{Kn} < 10^{-3}$ the continuity assumption with no slip boundary conditions is valid. In the slip regime, $0.01 < Kn < 0.1$, flow can be assumed to be continuous, but slip velocities will appear on the solid walls. For transitional and free molecular flow regimes, $Kn > 0.1$, the continuity assumption and therefore the validity of Navier-Stokes equation are under question. In these flows, the effect of solid walls causes the fluid behavior to be basically dependent on geometric dimensions (Arkilic *et al.* 1994).

Lattice-Boltzmann method, LBM, is an efficient method for simulation of fluid flows in porous media. This method is a particle-based mesoscopic method independent of actual number of molecules, so it has a low computational cost. In addition, LBM is more general than Navier-Stokes equations and holds true for a wider range of Knudsen numbers (Gad-el-Hak 1999).

Many researchers have used the LBM to simulate the gaseous flows in slip flow regime (Agrawal *et al.* 2005, Guo *et al.* 2006, 2007, 2008, Kim *et al.* 2005, Lee *et al.* 2005, Verhaeghe *et al.* 2009) but the efforts to simulate transitional flows have been limited (Shan *et al.* 2006, Chikatamarla *et al.* 2006, Ansumali *et al.* 2007, Kim *et al.* 2008, Zhang *et al.* 2006, Tang *et al.* 2008a, b). For the slip flow regime in porous media, Jeong *et al.* (2006) simulated the two-dimensional and three-dimensional flow passing through porous media for in-line and staggered geometries and Knudsen numbers of up to 0.1, and proposed an equation for permeability based on porosity and Knudsen number.

So far, only two methods have been proposed for simulation of transitional flows: one is based on high-order LBM (Shan *et al.* 2006, Chikatamarla *et al.* 2006, Ansumali *et al.* 2007, Kim *et al.* 2008) and the other is based on modification of mean free path length (Zhang *et al.* 2006, Tang *et al.* 2008a, b). High-order or multi-velocity LBM increases the order of accuracy for discretization of velocity phase space. Ansumali *et al.* (2007) showed that using high-order LBM improves the capabilities of the method, but Kim *et al* .(2008) argued that the high-order method can only predict the rarefaction effects of Knudsen numbers of the order of 0.1, and fails to predict the mass flow rate at large Knudsen numbers. In addition, high-order LBMs with large numbers of velocity directions are not numerically stable (Succi 2002). In nanoflows, the values of mean free path and characteristic length are closer to each other and the wall boundaries reduce the local mean free path. So Tang *et al.* (2008a, b) used a geometry dependent local mean free path to study the nonlinear high-order rarefaction, but this local mean free path is complicated and could not be used for complex geometries such as porous media.

To cover wide range of the flow regimes, (Homayoon *et al.* 2011, Shokouhmand and Meghdadi 2011) proposed a relaxation time formulation, named as modified LBM, by considering the rarefaction effect on the viscosity. The modified LBM was also utilized in some researches. For example, Zhuo and Zhong (2013) simulated the micro channel gas flows with a wide range of Knudsen numbers covering from the slip regime up to the entire transition regime via the D_2Q_9 LBM. For all test cases conducted in this study, the results are found to be in quite good agreement with the solutions of the linearized Boltzmann equation, the results of the DSMC and IP-DSMC methods. Also Liou and Lin (2013) performed numerical simulations on the pressure-driven rarefied flow through channels with a sudden contraction–expansion of 2:1:2 using D_2Q_9 and D_3Q_{19} lattice Boltzmann methods covering the slip and transition flow regimes. The numerically computed results are found to be in reasonably good agreement with the experimental ones. In another work, Li *et al.* (2011) used this effective relaxation time with a multiple relaxation time LBM to account for the rarefaction effect on gas viscosity. The results, including the velocity profile, the non-linear pressure distribution along the channel, and the mass flow rate, are in good agreement with the solution of the linearized Boltzmann equation, the direct simulation Monte Carlo, DSMC results, and the experimental results over a broad range of Knudsen numbers. Kalarakis *et al.* (2012) employed a single relaxation time model with this modified D_2Q_9 lattice Boltzmann method to simulate flow between parallel plates and flow in porous media. They tested the modified LB method against the DSMC method in the simple case of a straight channel. It was found that the velocity profiles were reproduced with reasonable accuracy for Knudsen numbers in the range of 0.1–10. In addition, the permeability predictions of the two methods for computer-aided reconstructions of porous media are in very good agreement with each other over the entire transition flow regime. They concluded that the modified D_2Q_9 LB method is suitable for prediction of the gas permeability in porous media over the entire slip and transition flow regimes.

Permeability k is a key variable to describe the transport capacity of a porous medium. The

permeability of a porous medium, for which there is no slip on the fluid-solid boundary, only depends on the porous structures. However, when the Knudsen number is relatively high, the gas slippage effect on solid boundaries occurs. Gas slippage in porous media and its effects on permeability was first studied by Klinkenberg (1941). It was found that due to the slippage phenomenon, the measured gas permeability (apparent permeability) through a porous medium is higher than that of the liquid (intrinsic permeability).

In the present work, by using this new relaxation time formulation, two-dimensional gas flows in porous structures with in-line and staggered arrangements is studied. This paper also presents a new equation for prediction of the permeability of nano porous structures in slip and transitional regimes.

2. MODIFIED LATTICE BOLTZMANN METHOD

The following is the continuum Boltzmann equation discretized in different velocity directions (Cercignani 1988):

$$\frac{\partial f_\alpha}{\partial t} + e_\alpha . \nabla f_\alpha = \mathbf{\Omega}_\alpha \tag{1}$$

where f is the particle distribution function, e_α is the microscopic velocity and $\mathbf{\Omega}_\alpha$ is the collision term. In D2Q9 model, space is discretized as a rectangular lattice with nine discrete velocities as shown below:

$$e_\alpha = \begin{cases} (0,0) & \alpha = 0 \\ (\cos[\frac{(\alpha-1)\pi}{2}], \sin[\frac{(\alpha-1)\pi}{2}])c & \alpha = 1-4 \\ (\cos[\frac{(\alpha-1)\pi}{2}+\frac{\pi}{4}], \sin[\frac{(\alpha-1)\pi}{2}+\frac{\pi}{4}])\sqrt{2}c & \alpha = 5-8 \end{cases} \tag{2}$$

where $c = \Delta x / \Delta t$, Δx is the lattice spacing and Δt is the time steps; here both Δx and Δt are set to 1. Using BGK collision operator, Eq. (1) yields to (Bhatnagar 1954):

$$f_\alpha(\mathbf{x} + \mathbf{e}_\alpha \Delta t, t + \Delta t) - f_\alpha(\mathbf{x}, t) = -\frac{1}{\tau}(f_\alpha(\mathbf{x}, t) - f_\alpha^{(eq)}(\mathbf{x}, t)) \tag{3}$$

The value of equilibrium distribution function can be calculated from the following equation:

$$\begin{aligned} f_\alpha^{eq} &= \frac{4}{9}\rho\left[1 - \frac{3}{2}u^2\right], \alpha = 0 \\ f_\alpha^{eq} &= \frac{1}{9}\rho\left[1 + 3(c_\alpha u) + \frac{9}{2}(c_\alpha u)^2 - \frac{3}{2}u^2\right], \alpha = 1,2,3,4 \\ f_\alpha^{eq} &= \frac{1}{36}\rho\left[1 + 3(c_\alpha u) + \frac{9}{2}(c_\alpha u)^2 - \frac{3}{2}u^2\right], \alpha = 5,6,7,8 \end{aligned} \tag{4}$$

The macroscopic flow variables such as density ρ and velocity u are then calculated in terms of the particle distribution function $f_\alpha(\vec{x}, t)$, by:

$$\rho = \sum_{\alpha=0}^{8} f_\alpha \tag{5}$$

$$\rho \mathbf{u} = \sum_{\alpha=0}^{8} \mathbf{e}_\alpha f_\alpha \tag{6}$$

In the standard Lattice Boltzmann Method, LBM, the relaxation time is related to the Knudsen number by the following relation (Nie 2002):

$$\tau = 0.5 + \sqrt{\frac{6}{\pi}} KnH \tag{7}$$

where H is the characteristic length. The performance of standard LBM with the relaxation time formulation of Eq. (7) is confined to the slip flow regime with a Knudsen number less than 0.1. To cover wide range of the flow regimes, by considering the rarefaction effect on the viscosity an effective relaxation time formulation, τ_{eff} , is proposed by Homayoon *et al.* (2011):

$$\tau_{eff} = 0.5 + (\frac{1}{1 + 2.2Kn}\frac{\rho}{\rho_{eff}})(\tau - 0.5) \tag{8}$$

The concept of effective relaxation time is based on the consideration that, when a wall is included in a gas flow system, in the near-wall region some gas molecules will hit the wall and their flight paths will be terminated by the wall, so that the local mean-free-path is smaller than that defined in unbounded systems. As a result, the gas viscosity and the relaxation time will be reduced (Li *et al.* 2001).

3. GEOMETRY AND BOUNDARY CONDITIONS

Porous structures shown in Fig. 1 are modeled by square obstacles, distributed with in-line and staggered arrangements in the flow field. Because of the periodicity of the porous geometry, it can be assumed that the porous structures used in this work consist of patterns which have been reproduced by repetition of the cells shown in Fig. 2.

The calculated permeability (in lattice units) under mesh refinement is shown in Table 1 for $\varepsilon = 0.885$ and $\mathrm{Kn}_o = 0.01$ which indicates that the lattice 366*366 is sufficient.

Table 1 Permeability under mesh refinement

lattice	366×366	732×732	1098×1098
K_{LB}	426.927	428.576	433.313

The inlet and outlet pressures are imposed using the method proposed by Lim *et al.* (2002). At the inlet and outlet boundaries, the unknown velocities u and v are computed from interior fluid nodes according

to the extrapolation method. After the extrapolation the unknown distribution functions are computed by the equilibrium distribution functions (Eq. (4)). For the entrance region the unknown boundary conditions are:

$$\begin{aligned} f_1(0,y,t) &= f_1^{eq}(\rho,u,v,0,y,t) \\ f_2(0,y,t) &= f_2^{eq}(\rho,u,v,0,y,t) \\ f_3(0,y,t) &= f_3^{eq}(\rho,u,v,0,y,t) \end{aligned} \quad (9)$$

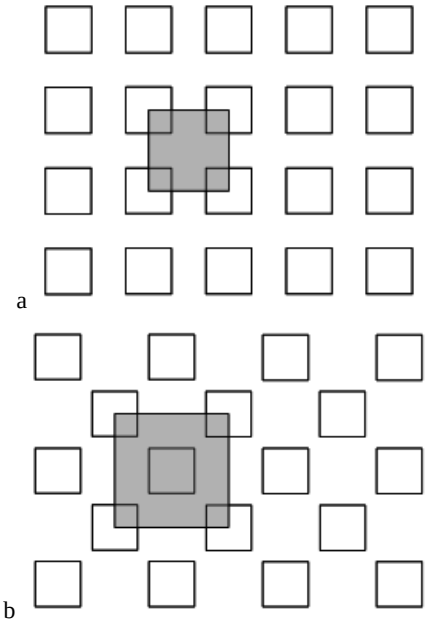

Fig. 1. Porous structure with square obstacles a) in-line structure, b) staggered structure.

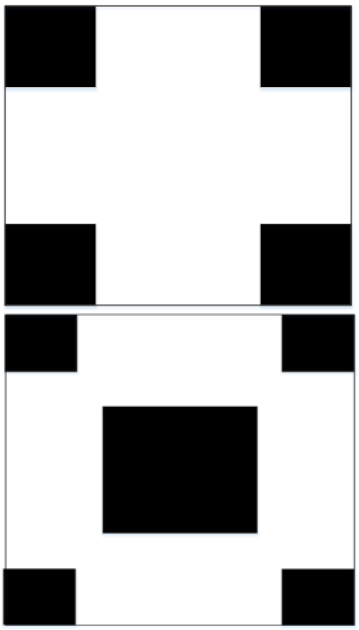

Fig. 2. Pattern of repetition cells.

For both in-line and staggered arrangements, the periodic boundary conditions are imposed at the top and bottom boundaries; meanwhile, the velocity slip on the solid walls is modeled with slip reflection boundary condition (Succi 2002). For example, at the lower boundaries, the unknown particle distribution functions f_2, f_5 and f_6, can be calculated as follows:

$$\begin{bmatrix} f_5(x,0) \\ f_2(x,0) \\ f_6(x,0) \end{bmatrix} = \begin{bmatrix} s & 0 & 1-s \\ 0 & 1 & 0 \\ 1-s & 0 & s \end{bmatrix} \begin{bmatrix} f_7(x+\delta x,\delta y) \\ f_4(x,\delta y) \\ f_8(x-\delta x,\delta y) \end{bmatrix} \quad (10)$$

where *s=0.7* is the slip-reflection coefficient on the solid wall.

The presented numerical method has been implemented on a FORTRAN 90 code. Which has been run on Intel® core(i7) CPU Q720 @ 1.60GHz. In all of the cases the convergence criteria is:

$$\frac{\sum_i \sum_j \left| \frac{u_{i,j}^{n} - u_{i,j}^{n-1}}{u_{i,j}^{n}} \right|}{NI \times NJ} \le 10^{-6} \quad (11)$$

where NI and NJ are the number of mesh elements in x and y directions respectively and the superscript n denotes the time step number.

4. RESULTS

According to the Darcy's law, for creeping flows, moving with a slow steady velocity (*Re<1*), the average velocity, U, is a linear function of pressure drop, as follow:

$$-\frac{dp}{dx} = \frac{\mu}{k} U \quad (12)$$

where k is the permeability. For pressure driven flows in micro/nano channels, using the second order slip boundary conditions, results in the following analytical solution for the corresponding volumetric flow rate (Tang *et. al.* 2005):

$$k = \frac{h^2}{12}\left(1 + 6C_1 Kn + 12C_2 Kn^2\right) \quad (13)$$

where h is the channel height and C_1 and C_2 are the first-order and second-order slip coefficients respectively.

For the micro/nano scale flows, the rarefaction effects lead to a nonlinear pressure drop resembling an incompressible flow (Karniadakis *et. al.* 2005). Therefore the gas permeability should be evaluated using the solution of compressible gas flows (Scheidegger *et. al.* 1972):

$$k = \frac{2\mu L u_o p_o}{{p_i}^2 - {p_o}^2} \quad (14)$$

where p_i, p_o, u_o and L are the inlet pressure, outlet pressure, outlet velocity and porous media length respectively.

The non-dimensional permeability, Darcy number,

can be estimated using the following relation:

$$Da = \frac{k}{D^2} \tag{15}$$

where D is the equivalent hydraulic diameter of the obstacles s defined as the $D = 4A/P$ where A is the obstacle area and P is the wetted perimeter. For higher Reynolds numbers (Forchheimer regime) the relationship is (Jeong *et al.* 2006):

$$-\frac{dp}{dx} = \frac{\mu}{k}U + C\rho|U|U \tag{16}$$

The parameter C is called the Forchheimer constant. Thus, the above equation may be rewritten as:

$$-\frac{dp}{dx} = DF.\frac{\mu U}{D^2} \tag{17}$$

where DF called as Darcy-Forchheimer drag, can be calculated by the following relation:

$$DF = \frac{D^2}{k} + \frac{D^2}{\mu}C\rho|U| \tag{18}$$

An experimental correlation for the flow through a packed bed of solid obstacles was proposed by Ergun (1952) that relates the DF drag to the flow and the porous medium parameters:

$$DF = C_1\frac{(1-\varepsilon)^2}{\varepsilon^3} + C_2\frac{(1-\varepsilon)}{\varepsilon^3}\mathrm{Re}_D \tag{19}$$

where $C_1 = 150$ and $C_2 = 1.75$ are model constants and porosity ε represents the fraction void volume in the porous structure as follows:

$$\varepsilon = \frac{V - V_s}{V} \tag{20}$$

Figure 3 presents the computed permeability in the slip flow regime of $Kn_o = 0.05$ for in-line and staggered arrangements. The figure shows a good agreement with the results of Jeong *et al.* (2006).

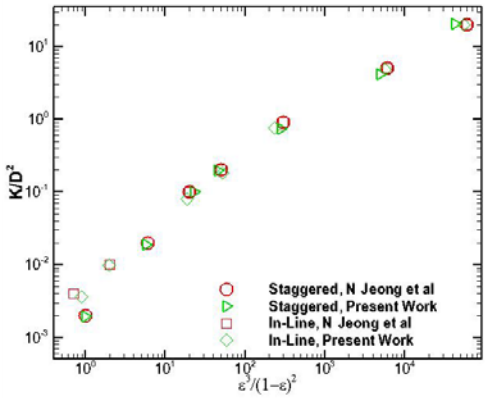

Fig. 3. Permeability obtained for Kn_o=0.05.

The DF drag for the in-line and staggered arrangements is presented in Fig. 4. The results of Jeong *et al.* (2006) are also presented for comparison. They are in close agreement which proves the validity of present work. It can be concluded from the figure that for the same Reynolds numbers, the DF drag of the staggered arrangement is higher than that of the in-line arrangement. This may be attributed to the fact that, for the in-line arrangement the pressure distribution in the narrow flow passage is similar to channel flow. For instance, Fig. 5 presents the pressure distribution and streamlines obtained for in-line and staggered porous structures. There exist high pressure stagnation regions in the staggered arrangement, while for the in-line arrangement the flow bears a resemblance to channel flow over open cavities. Also the figure shows that, for low pressure gradients ($\Delta\rho_{LB} = 0.001$) the creeping flow regime is observed, while in the Forchheimer flow regime, higher pressure gradient $\Delta\rho_{LB} = 0.1$ leads to vortex generation.

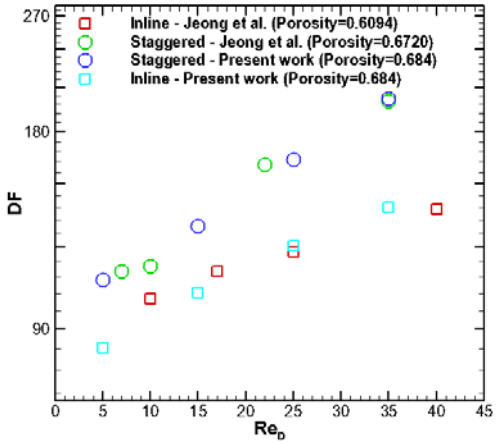

Fig. 4. Darcy-Forchheimer drag for the in-line and staggered arrangements.

Figure 6 shows the average velocity as a function of the pressure difference between the inlet and outlet for the in-line and staggered arrangements. The axes are in LB units. Since the Reynolds number is small, the curves are linear which indicates that the flow in porous media is in Darcian regime but for Kn=0.1 a little curvature can be observed in the figures which indicates that the flow approaches to the Forchheimer regime due to the increase in Reynolds number.

Figure 7 shows the estimated non-dimensional permeability in the slip and transitional flow regimes for the in-line and staggered arrangements. The Knudsen minimum effect can be observed. Increasing *Kn* causes the increase in velocity slip which leads to increase in flow rate in the slip flow regime (Kn<0.1). On the other hand increase in *Kn* causes the increase in the effective viscosity which leads to the decrease in flow rate. The net result is that by increasing the Knudsen number, the flow rate has a minimum value about *Kn≈0.4* and then it increases. This phenomenon is called Knudsen's minimum effect. For low Knudsen numbers (slip flow regime), the effect of higher order Kn in the Eq. (13) can be neglected, therefore the non-

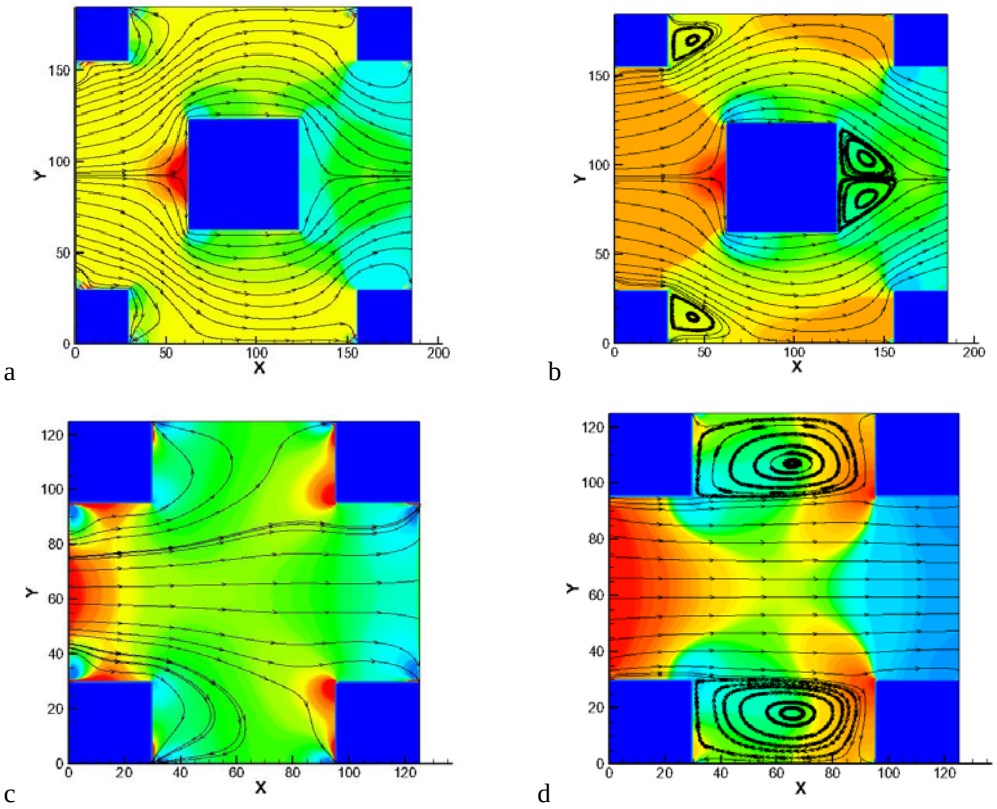

Fig. 5. Pressure distribution and streamlines for in-line and staggered porous structures a, c) $\Delta\rho_{LB} = 0.001$ b, d) $\Delta\rho_{LB} = 0.1$.

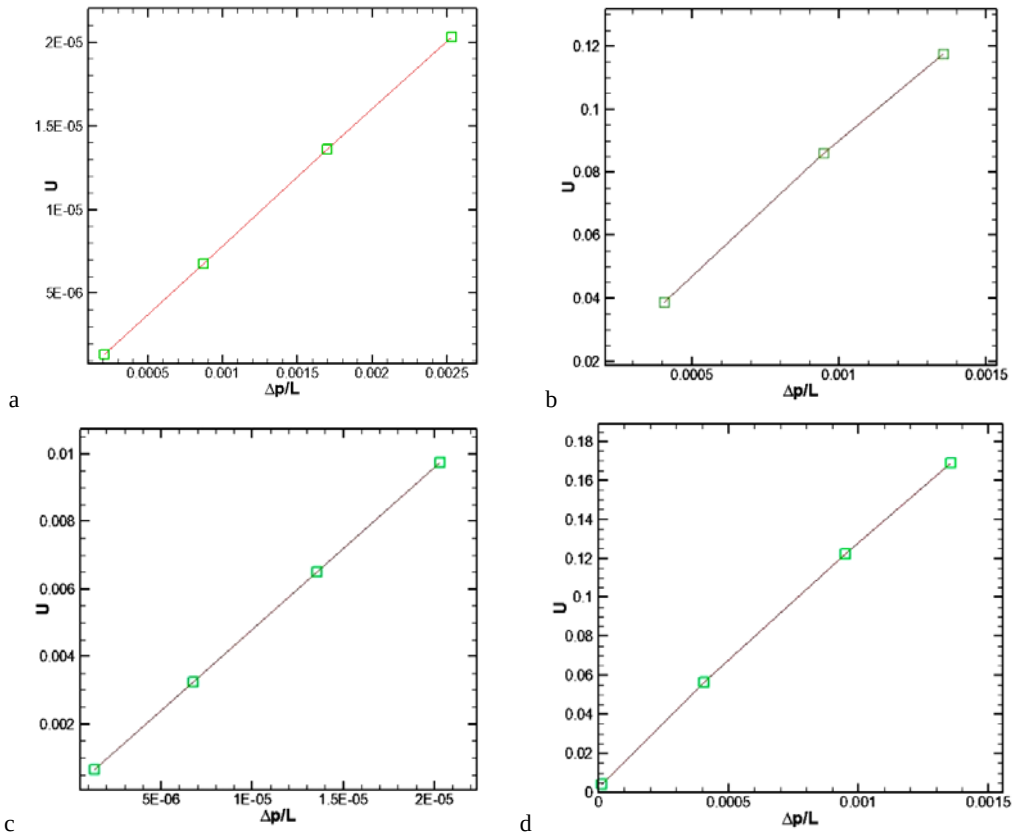

Fig. 6. Volume flow rate versus the pressure difference a) staggered Kn=0.05 b) staggered Kn=0.1 c) in-line Kn=0.05 d) in-line Kn=0.1.

dimensional permeability is a linear function of Kn while for the free molecular regime, the rate of increase in permeability decreases with increasing Kn_o. This is in consistent with the other numerical and experimental result for free molecular flow regime in micro and nano channels (Karniadakis *et. al.* 2005).

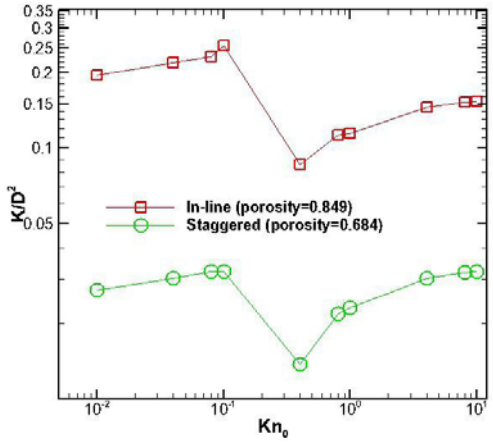

Fig. 7. Knudsen minimum effect in porous structures.

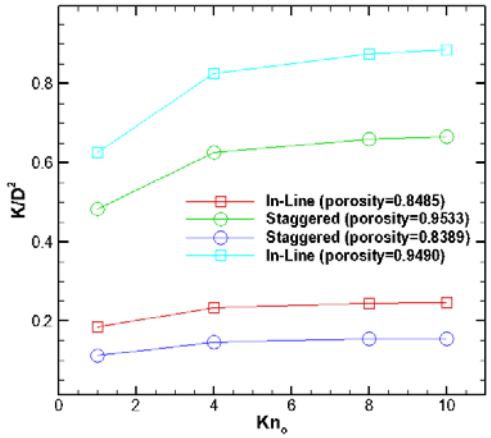

Fig. 8. Permeability versus Kn_o in transitional flow regime.

Figure 8 displays the porosity effect on the non-dimensional permeability in the transitional flow regime. By increasing the porosity, the obstacles decrease and the flow rate increases. Also, in the transitional regime, by increasing the Knudsen number, the permeability increases continuously. The rate of increase in the permeability is higher for higher porosities. It is also observed that the rate of increase is slightly larger for the in-line arrangement than that for the staggered arrangement. According to the fig. 8, despite of the fact that the porosity of the inline structure is less than that of the staggered one; the flow rate is higher. This phenomenon is related to existence of the high pressure stagnation regions in the staggered arrangement and less tortuosity (defined as the ratio of the flow path to the length scale) in the inline porous structure. By decreasing the tortuosity the pressure drop decreases and the permeability increases. It should be noted that the the computational time for the inline arrangement with $\varepsilon = 0.8485$ and Kn_o=1, is 1923 s.

Figure 9 presents the dimensionless permeability (k/D^2), which represents the first term of the Ergun correlation, versus $\varepsilon^3/(1-\varepsilon)^2$ for transitional flow regime of Kn=4. The abscissa is chosen so that the results can be directly compared with the Ergun correlation. The correlation of Ergun is also plotted in the figure for comparison. According to the figure, the results do not agree with the Ergun correlation. It may be concluded that the Ergun correlation is not applicable to porous media in transitional flow regime.

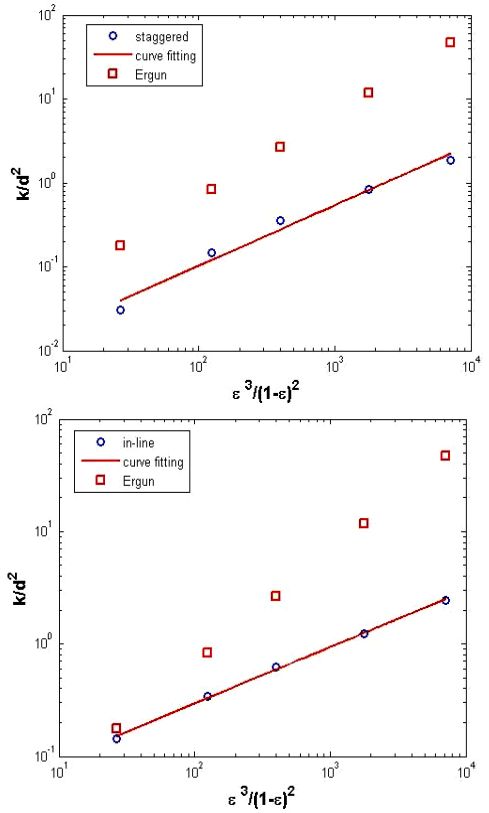

Fig. 9. Permeability against porosity for in-line and staggered structures.

Figures 10 and 11 show the non-dimensional permeability versus the porosity in transitional flow regime for in-line and staggered arrangements, respectively. With increasing the porosity ($\varepsilon^3/(1-\varepsilon)^2$), the obstacles decreases and the permeability increases.

In order to attain the correlation between the permeability and Kn_o data curve fitting is carried out for Kn_o =1, 4, 8, 10. According to the Figs. 10 and 11 a linear relation can be considered between $\ln(k/D^2)$ and $\ln(\varepsilon^3/(1-\varepsilon)^2)$. Therefore the resulting equation can be considered in the form of:

$$\frac{K}{D^2} = A\left[\frac{\varepsilon^3}{(1-\varepsilon)^2}\right]^B \tag{21}$$

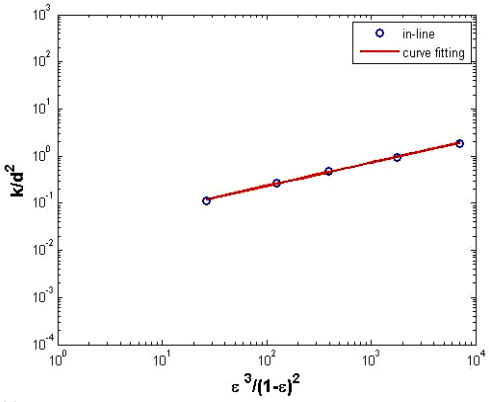

A) Kn=1

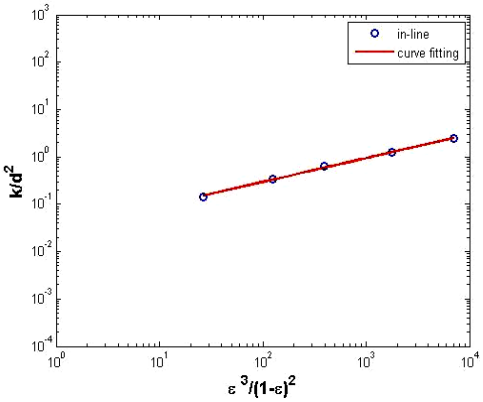

B) Kn=4

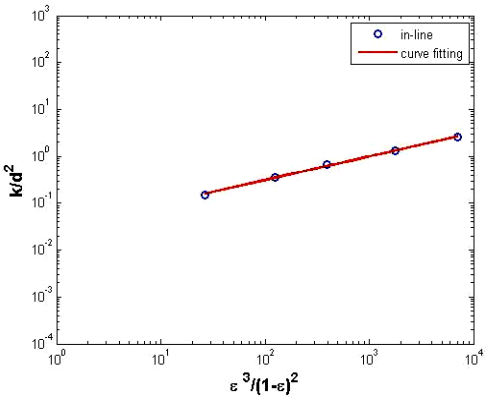

C) Kn=8

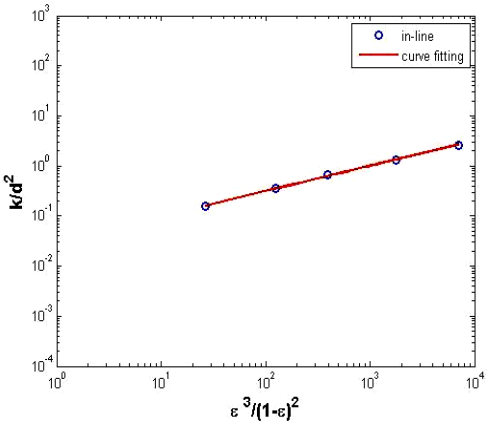

D) Kn=10

Fig. 10. Changes in porosity with respect to permeability for in-line porosity and different Knudsen numbers.

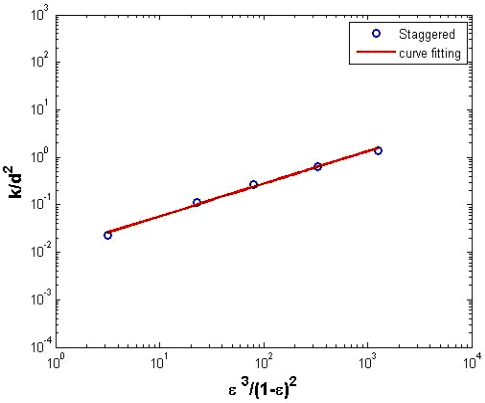

A) Kn=1

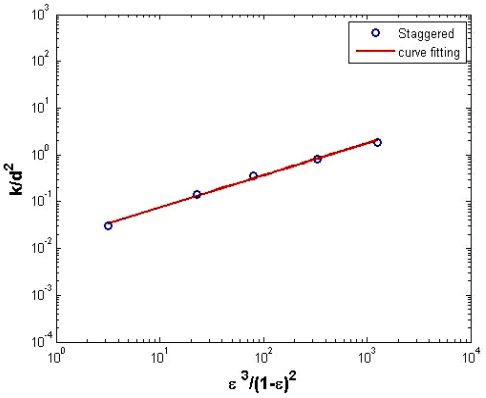

B) Kn=4

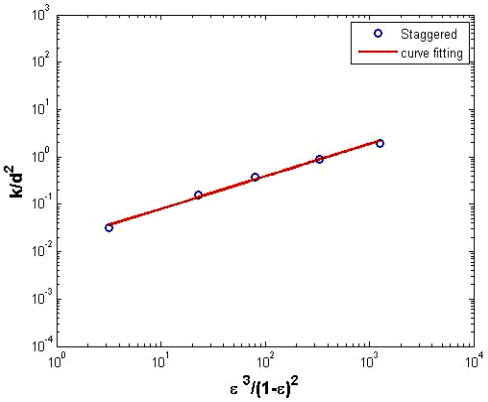

C) Kn=8

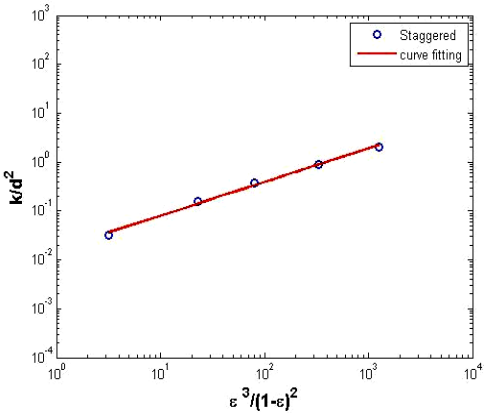

D) Kn=10

Fig. 11. Changes in porosity with respect to permeability for staggered porosity and different Knudsen numbers.

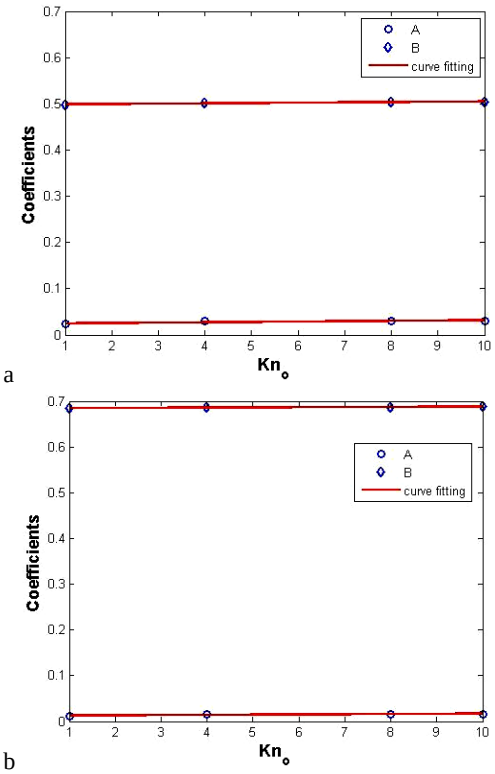

Fig. 12. Coefficients in the correlation of permeability for a) in-line b) staggered arrangements.

The coefficients A and B are functions of Kn_o, whose relationship can be curve fitted from the data exhibited in Table 2. Equation (22) presents the relations for coefficients A and B:

$$A=\begin{cases}0.00077795Kn_0+0.024 & \text{in-line}\\ 0.00046615Kn_0+0.0122 & \text{staggered}\end{cases}$$

$$B=\begin{cases}0.00069897Kn_0+0.4979 & \text{in-line}\\ 0.00038462Kn_0+0.6842 & \text{staggered}\end{cases} \quad (22)$$

Table 2 Coefficients A and B

Kn	In-line		staggered	
	A	B	A	B
1	0.0233	0.4972	0.0118	0.6843
4	0.0291	0.5026	0.0154	0.6863
8	0.0305	0.5037	0.0162	0.6872
10	0.0308	0.504	0.0163	0.688

Figure 12 shows the curves fitted to coefficients obtained for in-line and staggered geometries.

5. CONCLUSION

The nanoscale fluid flow in porous media with in-line and staggered patterns, is simulated by the modified Lattice-Boltzmann method assuming the dependence of the effective relaxation time on the local Knudsen number. The results obtained for slip regime demonstrated good agreement with the results of previous studies. The new permeability equation expressing the relationship between permeability, porosity and Knudsen number for transitional flow regime, is presented. This equation can be used to determine the permeability of porous media with in-line or staggered geometry for different Knudsen numbers. For the conditions considered, the following main results can be drawn:

- The DF drag of the staggered arrangement is higher than that of the in-line arrangement.
- In the slip flow regime, the non-dimensional permeability is a linear function of Kn, while for the free molecular regime, the rate of increase in permeability decreases with increasing Kn_o.
- In the transitional flow regime the permeability increases with increasing the Knudsen number and porosity, but the rate of increase in permeability is higher for higher Knudsen numbers.

REFERENCES

Agrawal, A., L. Djenidi and R. A. Antonia (2005). Simulation of gas flow in microchannels with a sudden expansion or contraction. *J. Fluid Mech*. 530, 135-144.

Ansumali, S., I. V. Karlin, S. Arcidiacono, A. Abbas and N. I. Prasianakis (2007). Hydrodynamics beyond Navier-Stokes: exact solution to the lattice Boltzmann hierarchy. *Phys. Rev. Lett*. 98(12).

Arkilic, E. B., K. S. Breuer and M. A. Schmidt (1994). Gaseous flow in microchannels. *ASME Winter Annual Meeting* 197, 57–65.

Assis, O. B. G. and L.C. Claro (2003). Immobilized lysozyme protein on fibrous medium: preliminary results for microfilteration applications. *Electron. J. Biotech*. 6(2), 161-167.

Bazant, M. Z. and T. M. Squires (2004). Induced-charge electrokinetic phenomena: Theory and microfluidic applications. *Phys. Rev. Lett*. 92(6).

Bhatnagar, P. L., E. P. Gross and M. Krook (1954). A model for collision processes in gases. *J. Phys. Rev*. 94, 511-525.

Biddiss, E., D. Erickson and D. Q. Li (2004). Heterogeneous surface charge enhanced micromixing for electrokinetic flows. *Anal. Chem*. 7(11), 3208-3213.

Brask, A., G. Goranovic, M. J. Jensen and H. Bruus (2005). A novel electro-osmotic pump design for nonconducting liquids: theoretical analysis of flow rate–pressure characteristics and stability. *J. Micromech. Microeng*. 15(4), 883-

891.

Cercignani, C. (1988). *The Boltzmann Equations and its Applications*. Springer-Verlag, New York.

Chen, L., L. Zhang, Q. Kang, H. S. Viswanathan, J. Yao, and W. Q. Tao (2014). Nanoscale simulation of shale transport properties using the lattice Boltzmann method: permeability and Knudsen diffusivity. *Sci. Rep*. 5, 8089.

Chen, L., Q. Kang, H. S. Viswanathan and W. Q. Tao (2014). Pore-scale study of dissolution induced changes in hydrologic properties of rocks with binary minerals. *Water Resour. Res.* 50(12), 9343-9365.

Chikatamarla, S. S. and I. V. Karlin (2006). Entropy and Galilean invariance of lattice Boltzmann theories. *Phys. Rev. Lett*. 97(19).

Dullien, F. A. L. (1991). *Porous Media: Fluid Transport and Pore Structure*, 2nd ed. (Academic, New York).

Ergun, S. (1952). Fluid flow through packed columns. *Chem. Eng. Prog*. 48, 89-94.

Gad-el-Hak, M. (1999). The fluid mechanics of microdevices. *J. Fluids Eng*. 12(1), 5-33.

Guo, Z. L., B. C. Shi, T. S. Zhao and C. G. Zheng (2007). Discrete effects on boundary conditions for the lattice Boltzmann equation in simulating microscale gas flows. *Phys. Rev. E* 76(5).

Guo, Z. L., C. G. Zheng and B. C. Shi (2008). Lattice Boltzmann equation with multiple effective relaxation times for gaseous microscale flow. *Phys. Rev. E* 77(3).

Guo, Z. L., T. S. Zhaoand, Y. Shi (2006). Physical symmetry, spatial accuracy, and relaxation time of the lattice Boltzmann equation for micro gas flows. *J. Appl. Phys*. 99(7).

Homayoon, A., A. H. Meghdadi Isfahani, E. Shirani and M. Ashrafizadeh (2011). A novel modified lattice Boltzmann method for simulation of gas flows in wide range of Knudsen number. *Int. Communications. Heat Mass Transfer* 38, 827-832.

Jeong, N., D. H. Choi and C. L. Lin (2006). Prediction of Darcy-Forchheimer drag for micro-porous structures of complex geometry using the lattice Boltzmann method. *J. micromech. Microeng.* 16, 2240-2250.

Kalarakis, A. N., V. K. Michalis, E. D. Skouras and V. N. Burganos (2012). Mesoscopic simulation of rarefied flow in narrow channels and porous media. *Transp Porous Med* 94, 385–398.

Karniadakis, G., A. Beskok and N. R. Aluru (2005). *Microflows and Nanoflows: Fundamentals and Simulation*. Springer.

Kast, W. and C. R. Hohenthanner, (2000). Mass transfer within the gas-phase of porous media. *Int. J. Heat Mass transfer* 43, 807-823.

Kim, S. H., H. P. Pitsch and I. D. Boyd (2008). Accuracy of higher-order lattice Boltzmann methods for microscale flows with finite Knudsen numbers. *J. Comput. Phys*. 227, 8655-8671.

Kim, W. T., M. S. Jhon, Y. Zhou, I. Staroselsky and H. D. Chen (2005). Nanoscale air bearing modeling via lattice Boltzmann method. *J. Appl. Phys*. 97(10).

Kiwi-Minsker, L. and A. Renken (2005). Microstructured reactors for catalytic reactions. *Catal. Today* 110(1), 2-14.

Klinkenberg, L. J. (1941). *The Permeability of Porous Media to Liquids and Gases.* American Petroleum Inst., Drilling and Productions practices, New York.

Lee, T. and C. L. Lin (2005). Rarefaction and compressibility effects of the lattice Boltzmann equation method in a gas microchannel. *Phys. Rev. E* 71(4).

Li, Q., Y. L. He, G. H. Tang and W. Q. Tao (2011). Lattice Boltzmann modeling of microchannel flows in the transition flow regime. *Microfluid Nanofluid* 10, 607-618.

Lim, C. Y., C. Shu, X. D. Niu, and Y. T. Chew (2002). Application of lattice Boltzmann method to simulate micro channel flows. *J. Phys. Fluids*. 14, 2299-2308.

Liou, T. M. and C. T. Lin (2013). Study on microchannel flows with a sudden contraction–expansion at a wide range of Knudsen number using lattice Boltzmann method. *Microfluid Nanofluid* 16(1-2), 315-327.

Nie, X., D. Doolen and S. Chen (2002). Lattice Boltzmann simulations of fluid flows in MEMS. *J. Stat. Phys*. 107(1-2), 279-289.

Oddy, M. H., J. G. Santiago and J. C. Michelsen (2001). Electrokinetic instability micromixing. *Anal. Chem*. 73, 5822-5832.

Roy, S., R. Raju, H. F. Chuang, B. A. Cruden and M. Meyyappan (2003). Modeling gas flow through microchannels and nanopores. J. *appl. Phys.* 93(8), 4870-4879.

Scheidegger, A. E. (1972). *The physics of flow through porous media*. 3rd ed. University of Torento press.

Shan, X., X. F. Yuan and H. Chen (2006). Kinetic theory representation of hydrodynamics: a way beyond Navier-Stokes equation. *J. Fluid Mech*. 550, 413–441.

Shokouhmand, H. and A. H. Meghdadi Isfahani (2012). An improved thermal lattice Boltzmann model for rarefied gas flows in wide range of Knudsen number. *Int. Communications Heat Mass Transfer 38(10), 1463-1469.*

Succi, S. (2002). Mesoscopic modeling of slip motion at fluid-solid interfaces with heterogeneous catalysis. *J. Phys. Rev. Lett.* 89(6).

Succi, S., I. V. Karlin and H. Chen (2002). Role of the H theorem in lattice Boltzmann hydrodynamic simulation. *Rev. Mod. Phys*. 74(4).

Tang, G. H., W. Q. Tao and Y. L. He (2005). Gas slippage effect on microscale porous flow using the lattice Boltzmann method. *phys. Rev. E* 72(5).

Tang, G. H., Y. H. Zhang and D. R. Emerson (2008). Lattice Boltzmann models for nonequilibrium gas flows. *Phys. Rev. E* 77(4).

Tang, G. H., Y. H. Zhang, X. J. Gu and D. R. Emerson (2008). Lattice Boltzmann modeling Knudsen layer effect in non-equilibrium flows. *EPL* 83(4).

Verhaeghe, F., L. S. Luo and B. Blanpain (2009). Lattice Boltzmann modeling of microchannel flow in slip flow regime. *J. Comput. Phys*. 228, 147-157.

Wong, P. K., J. T Wang, J .H. Deval and C. M. Ho (2004). Electrokinetics in Micro Devices for Biotechnology Applications. *IEEE/ASME Trans. Mechatron*. 9, 366-376.

Yuranov, I., A. Renken and L. Kiwi-Minsker (2005). Zeolite / sintered metal fibers composites as effective structured catalyst. *Appl. Catal*. 281(1), 55-60.

Zhang, Y. H., X. J. Gu, R. W. Barber .and D. R. Emerson (2006). Capturing Knudsen layer phenomena using a lattice Boltzmann model. *Phys. Rev. E* 74(4).